Circular RNA hsa_circ_102209 promotes the growth and metastasis of colorectal cancer through miR-761-mediated Ras and Rab interactor 1 signaling

CHI LI
First Affiliated Hospital of Jinzhou Medical University
Hong Zhou (zhhsp1@126.com)
First Affiliated Hospital of Jinzhou Medical University https://orcid.org/0000-0001-9200-9691

Primary research

Keywords: circRNA hsa_circ_102209, colorectal cancer, RIN1 signaling, growth, metastasis

Posted Date: April 20th, 2020

DOI: https://doi.org/10.21203/rs.2.24638/v2

Abstract

Background: The levels of hsa_circ_102209 in colorectal cancer (CRC) specimens and cells, as well as its effects on CRC cells were investigated.

Methods: The expression of hsa_circ_102209 in CRC and paired non-cancerous samples, human CRC and normal colonic epithelial cells were examined using reverse transcription-quantitative polymerase chain reaction (RT-qPCR). Cells with hsa_circ_102209 knockdown were established using lentiviral vectors. Cell proliferative ability was evaluated using CCK-8 assay; cell migration and invasion were assessed by wound healing and Transwell assay. Cell cycle arrest and apoptosis were determined; apoptosis and EMT markers were examined using RT-qPCR and western blotting. Tumour development and levels of associated proteins were determined in hsa_circ_102209 knockdown mice.

Results: Our results revealed that expression of hsa_circ_102209 was remarkably increased in CRC tissues, where the levels of miR-761 were notably reduced ($p<0.05$). Additionally, the levels of hsa_circ_102209 was associated with histology grade and occurrence of liver metastasis in CRC patients, and the expression of hsa_circ_102209 and miR-761 were negatively correlated ($p<0.05$). Moreover, hsa_circ_102209 was upregulated in CRC cells compared with normal colonic epithelial cells. Knockdown of hsa_circ_102209 notably inhibited the proliferation, migration, invasion and EMT of CRC cells ($p<0.05$), whereas enhanced cell cycle arrest at G0/G1 phase and apoptosis ($p<0.05$). Furthermore, miR-761/Ras and Rab interactor 1 (RIN1) axis was the putative target of hsa_circ_102209 in CRC and involved in hsa_circ_102209-modulated growth and metastasis in CRC cells ($p<0.05$). Knockdown of hsa_circ_102209 also remarkably suppressed tumor growth in vivo ($p<0.05$).

Conclusions: our data revealed that the expression of hsa_circ_102209 was elevated in CRC samples and cells. Furthermore, hsa_circ_102209 could promote the progression of CRC through miR-761/RIN1 axis. More importantly, hsa_circ_102209/miR-761/RIN1 signaling may be a novel therapeutic target for the treatment of CRC patients.

Background

Colorectal cancer (CRC) is one of the major causes of cancer-associated mortality, and ~1.4 million new cases are diagnosed globally each year (1). CRC is a multifactorial disease with complex pathogenesis, and previous reports have indicated that both genetic and epigenetic alterations are associated with the initiation and development of CRC (2-4). Modern therapeutic approaches have been developed in recent years (5,6), for instance, endoscopic and surgical resection are widely used for CRC patients. Nevertheless, the prognosis of this disease is still poor due to high occurrence of liver metastases (~50%), which is one of the main causes of CRC-related mortality (7,8). The therapeutic outcome of CRC patients is related to disease staging when he/she is diagnosed, and five-year survival rate for CRC patients with metastases remains poor (<10%) (9). Therefore, the molecular mechanisms underlying the development

of CRC need to be further investigated, and it is essential to discover promising diagnostic biomarkers for this disease.

Circular RNAs (circRNAs) are a new group of noncoding RNAs. Unlike their linear counterparts, circRNAs are characterized with a more stable structure by forming a continuous loop (10,11). As there are no free 5'-/3'- overhangs in circRNAs, they are resistant to exonuclease-mediated cleavage (12). In addition, circRNAs are specifically expressed in various tissues (13). Recently, some circRNAs have been revealed as novel gene regulators, but the potential roles of most circRNAs remain largely unknown and require further investigation (13). Previous studies have suggested that circRNAs may function as miRNA 'sponges' which competitively suppress the activity of miRNAs (14). Furthermore, circRNAs also contribute to the pathogenesis of numerous types of diseases, including nervous system disorders and cancer (15-17). Previous report has revealed the essential roles of a novel circRNA hsa_circ_0007534 in CRC, and it could promote the growth of cancer cells (18); however, the underlying mechanisms and putative downstream molecules of most circRNAs in CRC have not been completely elucidated.

MicroRNAs (miRNAs) are non-coding RNAs with the length of ~22 nt, which are potential downstream targets of other non-coding RNAs including lncRNAs and circRNAs (19,20). Previous reports have suggested that miRNAs exert their functions via binding to the 3' untranslated region of corresponding mRNAs (21,22). Aberrant expression profiles of miRNAs have been detected in patients with cancer, which leading to tumor development (23). For example, miR-93 induces the proliferation of glioma cells through phosphatidylinositol 3 kinase/protein kinase B signaling (22). Upregulated H19 could enhance cell proliferation via miR-675 in CRC (20). In addition, miR-140 and miR-152 interact with corresponding lncRNAs, consequently contributing to the progression of glioma (24,25). However, the potential functions of miRNAs in CRC remain elusive and require investigation. Among the abovementioned miRNAs, miR-761 is involved in the pathogenesis of gastric cancer by suppressing Ras and Rab interactor 1 (RIN1; 26).

In the present study, the effects of hsa_circ_102209-regulated signaling on the growth and metastasis of CRC cells were elucidated. Our data suggested that hsa_circ_102209 was upregulated in CRC tissues and cells. Knockdown of hsa_circ_102209 could inhibit the progression of CRC cells *in vitro*. In addition, miR-761/RIN1 axis was the putative target of hsa_circ_102209 in CRC and involved in hsa_circ_102209-modulated growth and metastasis in CRC cells. Knockdown of hsa_circ_102209 also remarkably suppressed tumor growth *in vivo*. In summary, our paper revealed the essential roles of hsa_circ_102209/miR-761/RIN1 signaling during the development of CRC, which could provide novel insight for the treatment of this disease.

Materials And Methods

CircRNA microarray. Total RNA was extracted using TRIzol reagent (Invitrogen; Thermo Fisher Scientific, Inc.) and RNeasy Mini Kit (Qiagen, Germany). Fluorescence-labelled targets were generated for circRNA array. Human circRNA array v2 (CapitalBio Technology) was designed, ~5,000 genes were mounted onto

the chip, the target sequences of these circRNAs were obtained from Rybak-Wolf 2015 and Circbase. Briefly, labeled targets were hybridized with the samples, which were scanned using Agilent Microarray Scanner (Agilent Technologies, Santa Clara, CA, USA). Data were normalized according to Quantile algorithm. Arrays were carried out using the protocol provided by Agilent Technologies Inc. Shanghai Corporation. Genes whose fold change >2 were further analyzed. Five most up- or down-regulated circRNAs in CRC patients were listed in Table I. Hsa_circ_102209 was selected for further study.

Clinical specimens. Fifty-six CRC and matched para-carcinoma tissues (≥5 cm from tumor margin; aged 40-78 years old; 26 males and 30 females) were obtained at the First Affiliated Hospital of Jinzhou Medical University (Jinzhou, China) during May 2010-March 2013. After surgery, the specimens were immediately frozen in liquid nitrogen and stored at -80˚C until further use. Prior to operation, none of the patients have received chemo- or radio-therapy. Moreover, no malignancy was found in other organs. The levels of hsa_circ_102209 were categorized into low/high group using the mean value. The biopsies were examined by two independent pathologists, and the clinicopathological features of enrolled patients were summarized in Table II. Overall survival rates were analyzed by the Kaplan-Meier method. Written informed consents were obtained from all the patients, and all the samples were kept anonymized. The experimental protocol was approved by the Medical Ethics Committee of the First Affiliated Hospital of Jinzhou Medical University.

Cell culture. One normal human colonic epithelial cell (NCM460) as well as five human CRC cell lines (SW48, P6C, HT-29, TC71 and Gp2d) were obtained from the American Type Culture Collection (Manassas, VA, USA). Cells were cultured in Dulbecco's modified Eagle's medium (DMEM) containing streptomycin (100 μg/ml), penicillin (100 U/ml) and 10% fetal bovine serum (FBS; HyClone; GE Healthcare Life Science). Cells were cultured at 37˚C in a humidified atmosphere supplemented with 5% CO_2.

Transfection. In order to generate hsa_circ_102209 or RIN1 overexpression model, wildtype (o/e-102209 or o/e-RIN1) as well as mutant (o/e-NC) fragment was constructed into PLCDH-cir vector (Ribobio, Guangzhou, China). The lentiviral vector was obtained from Hanbio (Shanghai, China). Transfection was carried out according to the manufacturer's protocols. CRC cells were selected by 0.5ug/mL puromycin (Sigma-Aldrich, St Louis, MO, USA) two weeks post-transfection. To establish the hsa_circ_102209 knockdown model, pooled siRNA targeting hsa_circ_102209 (si-102209) and negative control (si-NC) were purchased from Genepharm Co. Ltd. (Shanghai, China). The mimics/inhibitors of miR-761 and corresponding negative control (NC) were synthesized by Genepharm Co. Ltd. (Shanghai, China). The mimics/inhibitors (100pM) and siRNA (50nM) were transfected into CRC cells using Lipofectamine®2000 (Invitrogen; Thermo Fisher Scientific, Inc.) according to the manufacturer's protocols. At 8h following

transfection, the culture medium was replenished with fresh DMEM supplemented with 10% FBS. The transfection efficiency was evaluated using RT-qPCR.

Reverse transcription-quantitative polymerase chain reaction (RT-qPCR). RT-qPCR was used to examine the expression levels of hsa_circ_102209, miR-761 and RIN1 in each experimental group. MiRNA was isolated using miRNeasy Mini Kit (Qiagen, Shenzhen, China). TaqMan MicroRNA Assay (Applied Biosystems, Foster City, CA, USA) was used to determine the levels of miR-761, and qPCR was performed on Applied Biosystem 7500 (Foster City, CA, USA). Total RNA from clinical samples or cell lines was extracted using TRIzol® reagent (Invitrogen; Thermo Fisher Scientific, Inc.) according to the manufacturer's protocols. The concentration of eluted RNA was determined by NanoDrop 1000 spectrophotometer (Thermo Fisher Scientific, Inc.). Subsequently, cDNA was synthesized using a PrimeScript™ RT kit (Takara Biotechnology Co., Ltd., Dalian, China), and qPCR was carried out using SYBR Green PCR Master Mix (TaKaRa Biotechnology Co., Ltd.) according to the manufacturer's protocols. Endogenous GAPDH and U6 were used as controls to normalize the expression of mRNA and miRNA. The sequences of forward and reverse primer used in the experiment were as follows: hsa_circ_102209, 5'-GTGCAGAGAACTACATGTCACC-3' and 5'-TAAAGGGTTGTCGCAGTGTG-3'; miR-761, 5'-ACAGCAGGCACAGAC-3' and 5'-GAGCAGGCTGGAGAA-3'; RIN1, 5'-GCACCTGGCGAGAGAAAAG-3' and 5'-TAGATTTCCGCACGAGGA ACG-3'; GAPDH, 5'-GCAAGAGCACAAGAGGAAGA-3' and 5'-ACTGTGAGGAGGGGAGATTC-3' and U6, 5'-CTCGCTTCGGCAGCACATA-3' and 5'AACGATTCACGAATTTGCGT-3'. For thermocycler, PCR program used was as follows: 95˚C for 5 min, then 45 cycles of 95˚C for 15s, 60˚C for 20s and 72˚C for 10s. Relative expression was analysed using $2^{-\Delta\Delta Cq}$ method.

Northern blotting. Total RNA was extracted with TRIzol®. Equal amount of RNA (30 μg) was added onto 15% TBE-urea gels and separated using a 15% urea-PAGE gel. Then samples were transferred onto positively charged nylon membranes (GE Healthcare Life Sciences) and cross-linked with UV irradiation. The blots were hybridized with DIG-labelled probe for miR-761 (Exiqon, Denmark) at 42˚C overnight. Later on, the membranes were rinsed in low-stringency buffer (2xSSC containing 0.1% SDS). Then the levels of miRNAs were evaluated using a DIG Luminescent Detection Kit (Roche). U6 was used as a loading control.

Western blot analysis. Total protein from clinical samples or cells was extracted with radioimmunoprecipitation assay buffer (Beyotime Institute of Biotechnology, Shanghai, China). Protein concentration was measured using bicinchoninic acid assay (Beyotime Institute of Biotechnology). A total of 30 μg protein samples were loaded onto SDS-PAGE gel and separated. The protein was subsequently transferred to a PVDF membrane (EMD Millipore, Billerica, MA, USA). The membranes were

then blocked with tris-buffered saline (TBS) containing 5% skimmed milk at room temperature for 1 h, followed by incubation using primary antibodies: RIN1 (1:200; cat. no. ab9485; Abcam Biotechnology Inc.) or GAPDH (1:1,000; cat. no. sc-47724; Santa Cruz Biotechnology Inc.) at 4˚C overnight. The following day, the membranes were probed with horseradish peroxidase-conjugated secondary antibody (1:5,000; cat. no. sc-2371 or sc-2357; Santa Cruz Biotechnology Inc.) at room temperature for 2 h. The protein bands were visualized using an enhanced chemiluminescence protein detection kit (Pierce Biotechnology; Thermo Fisher Scientific, Inc), and the signal was quantified using Image J (NIH, Bethesda, MD, USA).

Assessment of cell viability. The cells were harvested 24 h post-transfection. The amount of cells seeded onto a 96-well plate was $3x10^4$/well. Cell viability was determined using CCK-8 assay (Dojindo Molecular Technologies, Inc., Kumamoto, Japan) at day 1, 2, 3 and 4 after inoculation. Briefly, 10 µl of CCK-8 solution was added in each well at different time points. After the incubation at 37˚C for another 2 h, the absorbance (450 nm) was measured by a microplate reader (Bio-Rad Laboratories, Inc., Hercules, CA, USA).

Cell migration assay. The migratory ability of cells was evaluated using a wound healing assay. Cells were seeded onto 6-well plates with a density of $2x10^5$ cells per well, and subsequently transfected with corresponding vectors. After the cell confluency reached ~90%, the monolayer of cell was scratched in a straight line using a sterile micropipette tip. Then the cells were washed three times with PBS and replenished with fresh culture medium. Later on, the changes of scratch width were monitored after the scratch at 6, 12 and 24 h. The images were acquired by an inverted microscope (magnificationx100, Olympus Corporation, Tokyo, Japan). Cell migration was determined using ImageJ 6.0 with the following formula: Migration area ratio = the proportion of closed wound area/the whole field of view area.

Cell invasion assay. The invasive activity of cells was examined using a Transwell assay. A total of $2x10^5$ cells were suspended in FBS-free medium and placed onto the Matrigel®-pre-coated (Sigma-Aldrich, St. Louis, MO, USA) upper chamber (BD Biosciences, Franklin Lakes, New Jersey, USA). Then, 500 µl of culture medium supplemented with 10% FBS was added into the lower counterpart. After overnight incubation, non-invasive cells were removed by a cotton swab, whereas cells invaded into the lower chamber were fixed by paraformaldehyde (4%) and subsequently stained using crystal violet (0.5%). The numbers of invasive cells were counted in five randomly selected fields using an inverted light microscope (magnificationx200, Olympus Corporation, Tokyo, Japan).

Analysis of cell cycle distribution and apoptosis. Cells treated with o/e-102209 or o/e-NC were seeded onto 6-well plates at a density of $2x10^5$ cells/well following. Later on, cell suspension was spun down using a low-speed centrifugation (1000rpm) at 4˚C for 5 mins. Cell pellets were rinsed and re-suspended using PBS, subsequently fixed with pre-chilled ethanol (70%) and left in the cold room (4˚C) for two days. Before being subjected to flow cytometry, cells were lysed, centrifuged and then re-suspended in propidium iodide (PI, Sigma-Aldrich, USA) staining buffer containing PI (50 μl/ml) and RNase A (250 μl/ml). Cell cycle distribution was examined using a flow cytometer (BD Biosciences, USA), and then the results were analysed by Flowjo version 7.6 software (Flowjo LLC, USA). To assess cell apoptosis, the cell suspension was incubated at 4˚C in dark for 30 mins and stained using 5 μl annexin V-FITC (JingMei Biotech, Beijing, China). Cell apoptosis was examined by a flow cytometer (BD Biosciences, USA) and then analysed using Flowjo version 7.6 software (Flowjo LLC, USA).

Animal model. Female BALB/C nude mice (4 to 5 weeks old) with the weight of 18 to 20 g were obtained from the Laboratory Animal Research Centre of Jinzhou Medical University (Jinzhou, China). The mice were housed under a temperature- (22±2˚C) and humidity-controlled (60%) atmosphere, with a 12-h dark/light cycle and libitum access to food/water for at least three days before the operation. Mice were randomly divided into two groups (n=5/group) and injected with SW48 cells transfected with si-NC or si-hsa_circ_102209. Briefly, $2x10^7$ cells were well suspended using 200μl PBS and then subcutaneously injected into the back of mice. Mice who developed tumors were closely observed at least four times/week. Six weeks following injection, the mice were sacrificed and tumor tissues were isolated. The volume of tumour was calculated using the formula: V (mm^3) =(length x $width^2$)/2. To induce the metastasis, $1x10^5$ cells were suspended using 20 μl PBS and then injected into the lateral tail vein of mice. After the inoculation, mice were randomly sorted into experimental groups which will be assessed 42 days later. The protocol of the present study was approved by Ethics Committee of the First Affiliated Hospital of Jinzhou Medical University.

Bioinformatic prediction. Targetscan (www.targetscan.org/) and miRanda (www.microrna.org/microrna/) were used to predict the putative targets of hsa_circ_102209 or miR-761. For the luciferase reporter assay, wildtype (WT) fragment of the 3’UTR of hsa_circ_102209/RIN1 with potential complementary sites of miR-761 were purchased from Shanghai GenePharma Co., Ltd. (Shanghai, China). They were constructed into pmirGLO Dual-Luciferase miRNA Target Expression Vector (Promega Corporation, Madison, WI, USA) according to the manufacturer's protocols. hsa_circ_102209/RIN1-3'UTR-MUT reporter plasmid that carried the mutant miR-761 binding site was also produced using QuikChange Multi Site-Directed Mutagenesis Kit (Stratagene, La Jolla, CA, USA). Subsequently, the corresponding vectors were used to co-transfect DH5α competent cells with miR-NC or miR-761 mimics. Then, luciferase activity was examined 48 h post-transfection using Dual Luciferase Reporter Assay System (Promega) according to the manufacturer’s protocols, and firefly luciferase activity was normalized to *Renilla* luciferase.

RNA-pull-down assay. Biotinylated miR-761-WT, miR-761-Mut together with negative control (GenePharma, Shanghai, China) were produced. Cells were harvested and lysed after 48 h. Cell lysates were indicated with Dynabeads M-280 Streptavidin. The beads with immobilized miR-761 were treated using 10mM ethylenediaminetetraacetic acid. TRIzol® was used to extract the bound RNAs, which were further subjected to RT-qPCR.

Statistical analysis. Data were presented as means ± standard error of the mean and interpreted using SPSS 17.0 (SPSS, Inc., Chicago, IL, USA). The significance of differences within groups was analysed using Student's t-test or one-way analysis of variance (ANOVA). Moreover, A student-Newman-Keuls test was carried out after ANOVA. The relationship between relative RNA levels was examined by Spearman's correlation analysis. Overall survival was examined using Kaplan-Meier survival test, and log rank test was used to compare the survival. Chi square test was used to evaluate the relationships among categorical variables. $P<0.05$ was considered to indicate a statistically significant difference.

Results

The level of hsa_circ_102209 is elevated in CRC samples and cell lines. The expression levels of hsa_circ_102209 were examined in 56 CRC samples and matched para-carcinoma tissues by RT-qPCR. Our data revealed that hsa_circ_102209 was significantly upregulated in CRC tissues compared with para-carcinoma controls (Fig. 1A). Furthermore, the association between hsa_circ_102209 and the progression of CRC was investigated, and the results suggested that the level of hsa_circ_102209 was remarkably increased in patients with advanced CRC (Fig 1B). In addition, the level of hsa_circ_102209 was notably elevated in CRC individuals with liver metastasis (Fig. 1C). Moreover, CRC patients with high expression levels of hsa_circ_102209 exhibited poor overall survival ($p=0.0025$, log-rank test; Fig. 1D) compared with the low expression counterpart. Additionally, upregulation of hsa_circ_102209 was also detected in all five CRC cell lines compared with normal colonic epithelial cells (Fig.1E). In summary, the expression of hsa_circ_102209 was significantly upregulated in CRC, which may also result in the tumour development.

Knockdown of hsa_circ_102209 suppresses the growth, metastasis and EMT of CRC cells. To study the influences of hsa_circ_102209 on the biological behaviors of CRC cells, the expression of hsa_circ_102209 was knockdown in SW48 and Gp2d cells. Transfection efficiencies were determined by RT-qPCR (Fig. 2A). In addition, the data of CCK-8 assay indicated that the proliferative activity of CRC cells transfected with si-hsa_circ_102209 was remarkably inhibited (Fig. 2B and C). Furthermore, would healing and Transwell assays were carried out to evaluate cell migration and invasion, respectively. The results revealed that cell migration and invasion were inhibited following the knockdown of hsa_circ_102209 expression compared with the control (Fig. 2D-G). Additionally, in order to investigate

the effects of hsa_circ_102209 knockdown on EMT of CRC cells, the expression levels of relevant markers including E-cad, vimentin and snail were examined. The protein and mRNA levels of abovementioned molecules were affected after the transfection with si-hsa_circ_102209 (Fig. 2H and I). Taken all together, knockdown of hsa_circ_102209 could lead to downregulated proliferation, migration, invasion and EMT of CRC cells.

Downregulated hsa_circ_102209 enhances cell cycle arrest and apoptosis in CRC cells. Based on the abovementioned findings, hsa_circ_102209 may be involved in the proliferation and metastasis of CRC cells *in vitro*. To further determine the influences of hsa_circ_102209 knockdown, cell cycle distribution and apoptosis in transfected CRC cells were also examined compared with the control. Our data suggested that CRC cell cycle was notably shifted from S and G2/M to G0/G1 phase. Furthermore, the cell proportion of G0/G1 phase was significantly elevated, while that in S phase was remarkably decreased (Fig. 3A and B). In addition, the results of flow cytometry indicated that knockdown of hsa_circ_102209 increased the apoptosis rate of CRC cells (Fig. 3C), which was further confirmed by the upregulation of apoptosis-associated molecules such as Bax, Cas-9 and MMP9 (Fig. 3D and E). In summary, these data revealed that hsa_circ_102209 knockdown may arrest cell cycle in G0/G1 phase and consequently promote the apoptosis of CRC cells.

MiR-761 is the novel downstream molecule of hsa_circ_102209 *in CRC.* To investigate whether hsa_circ_102209 is a putative oncogene in CRC and its roles via targeting downstream miRNAs, the potential targets of has_circ_102209 were predicted using bioinformatics approaches, including miR-761, miR-197-3p, miR-204-5p, miR-211-5p and miR-134-5p. Among them, the 3'-UTR of miR-761 contained a highly conserved binding site for has_circ_102209 (Fig. 4A). Moreover, the relationship between hsa_circ_102209 and miR-761 was confirmed by luciferase activity assay. The plasmids carrying wild-type (WT-hsa_circ_102209) and mutant (MUT-hsa_circ_102209) sequence of predicted miR-761 complementary sites were produced. The results indicated that miR-761 mimics remarkably decreased the activity of WT-hsa_circ_102209 luciferase reporter by comparing to the control (Fig. 4B). The RNA-pull-down assay revealed that hsa_circ_102209 was enriched in biotin-labeled miR-761-WT group (Fig. 4C). Additionally, the data of RT-qPCR and northern blotting revealed that the expression level of miR-761 was downregulated in CRC tissues (Fig. 4D and E). Furthermore, downregulation of miR-761 was observed in SW48 and Gp2d cells (Fig. 4F and G).

In order to further investigate the influences of hsa_circ_102209 on the expression of miR-761, SW48 cells were co-transfected with o/e-102209 and miR-761 mimics, or with si-hsa_circ_102209 and miR-761 inhibitors, respectively. The transfection efficiencies were confirmed using RT-qPCR (Fig. 5A-C). The results of northern blot analysis also suggested that the upregulation of miR-761 in SW48 cells transfected with miR-761 mimics was abolished by o/e-102209 (Fig. 5D). Vice versa, downregulation of miR-761 in SW48 cells transfected with miR-761 inhibitors was reversed after co-transfection with si-hsa_circ_102209 (Fig. 5E). Furthermore, the association between hsa_circ_102209 and miR-761 was further determined by Spearman's correlation analysis, and the results suggested that the expression levels of miR-761 and hsa_circ_102209 were inversely correlated in CRC tissues (Fig. 5F).

RIN1 is a potential target of miR-761 in CRC. To identify the putative downstream molecule of miR-761, bioinformatics study was performed and several pathways were identified. Among them, miR-761 is able to inhibit RIN1 signaling and regulate the development of gastric cancer (26), thus it is selected for further study. The complementary sequence between miR-761 and RIN1 transcripts was predicted (Fig. 6A). The relationship of RIN1 and miR-761 was also revealed by luciferase assay. The vectors containing the wild-type (WT-RIN1) and mutant (MUT-RIN1) sequence of predicted miR-761 binding sites were generated. The results indicated that overexpression of miR-761 significantly suppressed the activity of luciferase reporters carrying WT-RIN1 sequence but not in the one with mutant (Fig. 6B). The RNA-pull-down assay indicated that RIN1 was enriched in biotin-labeled miR-761-WT group (Fig. 6C). In addition, the results of RT-qPCR suggested that the level of RIN1 was increased in CRC tissues compared to normal controls (Fig. 6D). Furthermore, upregulation of RIN1 was observed in both SW48 and Gp2d cells (Fig. 6E and F). Moreover, the expression levels between RIN1 and miR-761 were negatively correlated in CRC samples (Fig. 6G). The expression level of RIN1 was remarkably increased in CRC cells treated with o/e-102209; significant downregulation of RIN1 was detected following the transfection with miR-761 mimics, which was restored by overexpression of hsa_circ_102209 in CRC cells (Fig. 6H). In summary, hsa_circ_102209 could increase the expression level of RIN1 in CRC cells by sponging miR-761.

RIN1 could be involved in hsa_circ_102209-modulated biological behavior changes in CRC cells. In order to investigate whether hsa_circ_102209-mediated upregulation of RIN1 is associated with the development of CRC, CRC cells were transfected with control vector, o/e-RIN1 or co-treated with si-hsa_circ_102209. Transfection efficiencies were determined by RT-qPCR (Fig. 7A). In addition, CCK-8 assay revealed that the proliferation of CRC cells transfected with o/e-RIN1 was significantly promoted, which was abrogated by hsa_circ_102209 knockdown (Fig. 7B and C). Similarly, would healing and Transwell assays indicated that cell migration and invasion were enhanced by overexpressed RIN1, but these effects were notably reversed by the transfection with si-hsa_circ_102209 (Fig. 7D-G). Furthermore, the expression levels of EMT-associated molecules were also influenced by overexpression of RIN1, which was abolished after the transfection with si-hsa_circ_102209 (Fig. 7H and I).

Moreover, cycle distribution and apoptosis in transfected CRC cells were also determined. Our data revealed that cell cycle was shifted from G0/G1 to S and G2/M phase in CRC cells transfected with o/e-RIN1, which were reversed by knockdown of hsa_circ_102209 expression. In addition, the cell percentage of G0/G1 phase was remarkably reduced by o/e-RIN1, but these effects were abrogated by knockdown of hsa_circ_102209 (Fig. 8A and B). In addition, the results of flow cytometry suggested that overexpressed RIN1 inhibited the apoptosis of CRC cells, which was abolished by the transfection with si-hsa_circ_102209 (Fig. 8C). These findings were further confirmed by the changes of apoptosis-related markers including Bax, Cas-9 and MMP9 (Fig. 8D and E). Taken all together, the biological behavior changes caused by overexpressed RIN1 were abrogated by knockdown of hsa_circ_102209. These findings revealed that RIN1 is involved in hsa_circ_102209-mediated growth and metastasis in CRC cells, suggesting hsa_circ_102209/miR-761/RIN1 axis could contribute to the progression of CRC.

Knockdown of hsa_circ_102209 suppresses the development of CRC in vivo. In order to study whether si-102209 is able to inhibit the growth and metastasis of CRC *in vivo*, cells transfected with si-NC or si-102209 were subcutaneously injected into BALB/C nude mice. Six weeks post-inoculation, the mice were sacrificed and tumor tissues were isolated and further examined (Fig. 9A). The mean value of tumor volume in si-102209 group was remarkably reduced compared with the controls (Fig. 9B). In addition, the average tumor weight of hsa_circ_102209 knockdown mice was notably decreased (Fig. 9C). Furthermore, the numbers of macroscopic nodules were significantly reduced in si-102209 group (Fig. 9D). The results of western blotting also indicated that EMT-/apoptosis- related markers and RIN1 exhibited the same expression pattern as detected in the *in vitro* assays (Fig. 9E). Taken all together, our findings indicated that knockdown of hsa_circ_102209 is able to inhibit the progression of CRC *in vivo* possibly through downregulating RIN1.

Discussion

CRC is considered as the major cause cancer-related mortality, and ~1.4 million new cases are diagnosed globally every year (1). Recent research suggested that genetic/epigenetic alterations could trigger the progression of CRC (2-4). Moreover, the survival rate for CRC patients with metastases remains poor (<10%; 9). The detailed mechanisms underlying the pathogenesis of CRC are still unknown, therefore, it is urgent to discover novel diagnostic biomarkers for this disease. Recently, accumulating evidences have revealed that circRNAs could be key regulators during the progression of cancer. They may function as putative tumor promoters/suppressors, and impaired expression levels of circRNAs could lead to tumorigenesis (10-13). Additionally, circRNAs are able to function as “sponges’ of certain miRNAs, consequently inhibiting their activities (14). For example, circRNAs GLI2 could promote the growth of osteosarcoma by modulating miR-125b-5p (17). Furthermore, circRNA ZKSCAN1 is capable of suppressing the growth and metastasis of hepatocellular carcinoma cells (16). However, the underlying mechanisms and novel targets of circRNAs in CRC are not completely understood. Previous studies have suggested that miRNAs were associated with the pathogenesis of cancer (20-25). MiRNAs are promising oncogenic factor or tumor suppressors; they function as essential regulators of gene expression and are putative targets of circRNAs (19-24). For instance, miR-93 is able to enhance the proliferation of glioma cells by targeting phosphatidylinositol 3 kinase/protein kinase B pathway (22). In addition, miR-140 and miR-152 could interact with certain lncRNAs during tumourgenesis (24,25); however, the exact functions of miRNAs in CRC remain largely unknown and require further investigation. Among the abovementioned miRNAs, miR-761 is associated with the progression of gastric cancer by suppressing RIN1 (26).

In our paper, increased expression levels of hsa_circ_102209 were observed in CRC samples and cell lines. Knockdown of hsa_circ_102209 inhibited the growth and metastasis of CRC cells in vitro. In addition, function studies were conducted to investigate the downstream molecules and signaling of hsa_circ_102209 in CRC. Our data suggested that hsa_circ_102209 binds to miR-761, whose levels were notably reduced in CRC tissues and cells. Furthermore, the level of miR-761 was downregulated by hsa_circ_102209 in CRC cells, and their expression were negatively correlated in CRC samples. Similarly, it

has been reported that novel circRNA CDR1as suppresses the progression of CRC via miR-7 (27). Moreover, circRNAs including hsa_circ_0000523, ITCH and hsa_circ_0007142 are involved in the pathogenesis of CRC by regulating tumor cell growth (28-30). Furthermore, previous study has also revealed that hsa_circ_0007534 is involved in the development of gastric cancer by targeting Bcl-2 (18).

Additionally, RIN1 was identified as the putative target of miR-761, and its expression levels were notably increased in CRC samples and cells. The level of RIN1 was upregulated by hsa_circ_102209 and downregulated by miR-761 in CRC cells, respectively. Furthermore, the growth and development of CRC cells could be enhanced by overexpressed RIN1, and these effects were remarkably abrogated by hsa_circ_102209 knockdown. These data indicated that RIN1 could be involved in tumor cell growth and metastasis during the progression of CRC. In consistence with our findings, previous study has reported that miR-761 is associated with the development of gastric cancer by regulating RIN1 (26).

Conclusion

Our data revealed that hsa_circ_102209 was a novel oncogene in CRC that could promote the growth and metastasis of tumor cells by suppressing miR-761 and upregulating RIN1. The abovementioned findings revealed the key roles of hsa_circ_102209 on tumorigenesis and elucidated the potential mechanisms underlying its regulatory functions. Taken all together, our study indicated that hsa_circ_102209/miR-761/RIN1 axis could be associated with the progression of CRC. More importantly, and this novel signaling pathway could be a promising therapeutic target for the treatment of patients with CRC. For instance, miRNA-targeted therapy such as treatment with synthetic miR-761 mimics could be considered in future.

Abbreviations

CRC: colorectal cancer; Ras and Rab interactor 1; reverse transcription-quantitative polymerase chain reaction (RT-qPCR).

Declarations

Acknowledgements

Not applicable.

Funding

Not applicable.

Availability of data and materials

All the original datasets generated or analyzed in our study are available upon reasonable request.

Authors' contributions

CL and HZ designed this study. Both authors carried out the experiments and analyzed the data. CL and HZ drafted the original manuscript, reviewed and approved the final version of this manuscript.

Ethics approval and consent to participate

The protocol was approved by the Ethics Committee of the First Affiliated Hospital of Jinzhou Medical University (Jinzhou, China). Written informed consents were received from all patients prior to sample collection.

Patient consent for publication

Not applicable.

Competing interests

The authors declare that they have no competing interests.

References

1. Torre L, Bray F, Siegel R, Ferlay J, et al: Global cancer statistics. CA Cancer J Clin 65: 87-108, 2015.
2. Walther A, Johnstone E, Swanton C, Midgley R, et al: Genetic prognostic and predictive markers in colorectal cancer. Nat Rev Cancer. 9: 489–99, 2009.
3. Fearon E: Molecular genetics of colorectal cancer. Annu Rev Pathol. 6: 479-507, 2011.
4. March H, Rust A, Wright N, Hoeve J, et al: Insertional mutagenesis identifies multiple networks of cooperating genes driving intestinal tumorigenesis. Nat Genet 43: 1202-9, 2011.
5. D'Souza N, Robinson P, Branagan G, Chave H: Enhanced recovery after anterior resection: earlier leak diagnosis and low mortality in a case series. Ann R Coll Surg Engl. 20:1-6, 2019.
6. Sheikh L, Croft R, Harmston C: Counting the costs of complications in colorectal surgery. N Z Med J. 132: 32-36, 2019.
7. Fidler I: The pathogenesis of cancer metastasis: the “seed and soil” hypothesis revisited. Nat Rev Cancer. 3: 453-8, 2003.
8. Jemal A, Bray F, Center MM, Ferlay J, et al.: Global cancer statistics. CA Cancer J Clin. 61: 69–90, 2011.
9. Van C, Nordlinger B, Cervantes A: Advanced colorectal cancer: ESMO clinical practice guidelines for treatment. Ann Oncol Off J Eur Soc Med Oncol ESMO. 21: 93-97, 2010.
10. Memczak S et al. Circular RNAs are a large class of animal RNAs with regulatory potency. Nature. 495: 333–338, 2013.
11. Salzman J, Gawad C, Wang P, Lacayo N, Brown P. Circular RNAs are the predominant transcript isoform from hundreds of human genes in diverse cell types. Plos One, 7, e30733, 2012.

12. Vicens Q and Westhof E. Biogenesis of Circular RNAs. Cell. 159: 13-14, 2014.
13. Conn S. et al. The RNA binding protein quaking regulates formation of circRNAs. Cell. 160: 1125-1134, 2015.
14. Hansen T et al. Natural RNA circles function as efficient microRNA sponges. Nature. 495: 384-388, 2013.
15. You X et al. Neural circular RNAs are derived from synaptic genes and regulated by development and plasticity. Nat Neurosci. 18: 603-610, 2015.
16. Yao Z, Luo J, Hu K et al. ZKSCAN1 gene and its related circular RNA (circZKSCAN1) both inhibit hepatocellular carcinoma cell growth, migration, and invasion but through different signaling pathways. Mol Oncol. 11(4):422-437, 2017.
17. Li J and Song Y. Circular RNA GLI2 promotes osteosarcoma cell proliferation, migration, and invasion by targeting miR-125b-5p. Tumour Biol. 39(7), 2017.
18. Zhang R et al. Silencing of has-circ-0007534 suppresses proliferation and induces apoptosis in colorectal cancer cells. Eur Rev Med Pharmacol Sci. 22: 118-126, 2018.
19. Zhao X, Sun J, Chen Y, Su W, Shan H, Li Y, Wang Y, Zheng N, Shan H and Liang H: LncRNA PFAR promotes lung fibroblast activation and fibrosis by targeting miR-138 to regulate the YAP1-Twist axis. Mol Ther 26: 2206-2217, 2018.
20. Tsang WP, Ng EK, Ng SS, Jin H, Yu J, Sung JJ and Kwok TT: Oncofetal H19-derived miR-675 regulates tumor suppressor RB in human colorectal cancer. Carcinogenesis 31: 350-358, 2010.
21. Cimmino A, Calin GA, Fabbri M, Iorio MV, Ferracin M, Shimizu M, Wojcik SE, Aqeilan RI, Zupo S, Dono M, et al: miR-15 and miR-16 induce apoptosis by targeting BCL2. Proc Natl Acad Sci USA 102: 13944-13949, 2005.
22. Ohta K, Hoshino H, Wang J, Ono S, Iida Y, Hata K, Huang SK, Colquhoun S and Hoon DS: MicroRNA-93 activates c-Met/PI3K/Akt pathway activity in hepatocellular carcinoma by directly inhibiting PTEN and CDKN1A. Oncotarget 6: 3211-3224, 2015.
23. Liang Z, Feng Q, Xu L, Li S and Zhou L: CREPT regulated by miR-138 promotes breast cancer progression. Biochem Biophys Res Commun 493: 263-269, 2017.
24. Zhao H, Peng R, Liu Q, Liu D, Du P, Yuan J, Peng G, Liao Y: The lncRNA H19 interacts with miR-140 to modulate glioma growth by targeting iASPP. Arch. Biochem. Biophys. 610: 1-7, 2016.
25. Chen L, Wang Y, He J, Zhang C, Chen J, Shi D: Long non-coding RNA H19 promotes proliferation and invasion in human glioma cells by downregulating miR-152. Oncol. Res. 2018.
26. Zhang Q, Sui Y and Sui X: MicroRNA-761 inhibits the metastasis of gastric cancer by negatively regulating Ras and Rab interactor 1. Oncology Letters. 18: 3097-3103, 2019.
27. Tang W et al.: Silencing CDRlas inhibits colorectal cancer progression through regulating microRNA-7. Oncotargets and Therapy. 10: 2045-2056, 2017.
28. Zhu C et al.: Circular RNA has_circ_0007142 is upregulated and targets miR-103a-2-5p in colorectal cancer. Journal of Oncology. 2019.

29. Huang G et al.: Cir-ITCH plays an inhibitory role in colorectal cancer by regulating the Wnt/b-catenin pathway. PloS ONE, 10(6): e0131225, 2015.
30. Jin Y et al.: Circular RNA has_circ_0000523 regulates the proliferation and apoptosis of colorectal cancer cells as miRNA sponge. 51(12):e7811, 2018.

Tables

Table I. The top five up-/downregulated circRNAs in the array.

CircRNA ID	Fold change	p-value	circRNA type	Genomic location
Upregulated				
hsa_circ_102209	4.92	0.00672	exonic	chr22
hsa_circ_0000735	3.56	0.00721	exonic	chr17
hsa_circ_0023642	2.92	0.01123	exonic	chr11
hsa_circ_0068610	2.13	0.03015	exonic	chr3
hsa_circ_0032821	2.09	0.04234	exonic	chr14
Downregulated				
hsa_circ_0005730	3.17	0.04005	exonic	chr5
hsa_circ_0003645	3.02	0.02124	exonic	chr16
hsa_circ_0026134	2.86	0.01034	exonic	chr12
hsa_circ_0061274	2.32	0.01903	exonic	chr21
hsa_circ_0092368	2.11	0.00706	exonic	chr1

Table II. Clinicopathological parameters of CRC patients enrolled in this study.

Parameters	n	Hsa_circ_102209 expression		P value
		Low	High	
Gender				0.515
Male	26	13	13	
Female	30	15	15	
Age (years)				0.418
>60	24	12	12	
≤60	32	16	16	
Tumor size (cm)				0.404
>5	24	13	11	
≤5	32	15	17	
Histology grade				0.019*
I-II	34	12	22	
III-IV	22	16	6	
Smoking				0.433
Yes	31	15	16	
No	25	13	12	
Liver metastasis				0.012*
Yes	22	17	5	
No	34	11	23	

Differences among variable were analyzed using the $\chi 2$ test, * indicates that the values have statistically significant differences.

Figures

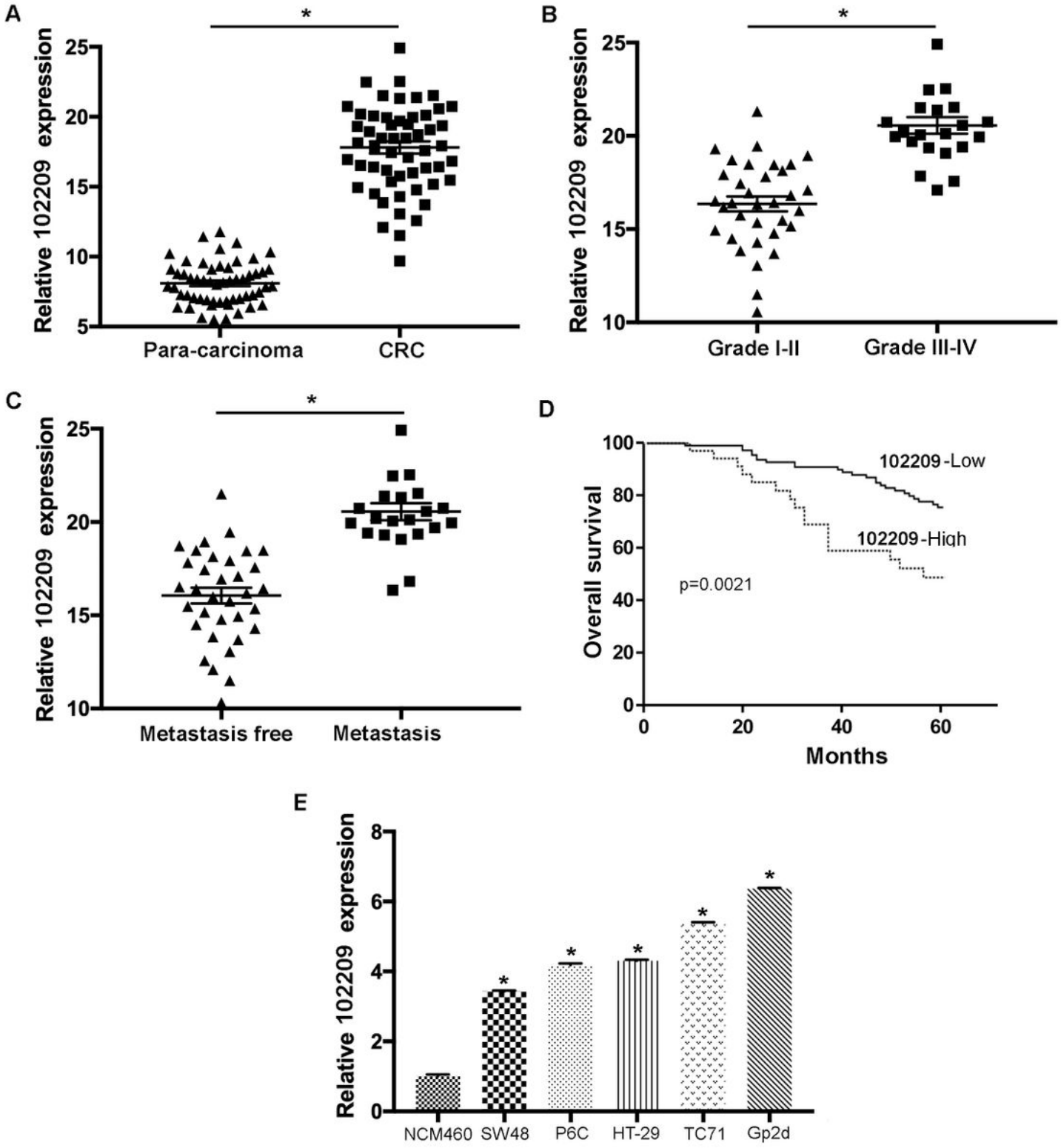

Figure 1

The level of hsa_circ_102209 is upregulated in CRC tissues and cells. (A) The expression of hsa_circ_102209 was examined in 56 CRC samples and matched para-carcinoma tissues by reverse transcription-quantitative polymerase chain reaction. (B) Hsa_circ_102209 expression was determined in CRC patients with various tumour grading. (C) The level of hsa_circ_102209 was assessed in CRC patients with metastasis compared with the control. (D) Survival analysis of CRC samples with relatively

low-/high-expression of hsa_circ_102209. (E) The expression of hsa_circ_102209 was examined in CRC cell lines compared to normal human colonic epithelial cells. *P<0.05. CRC, colorectal cancer.

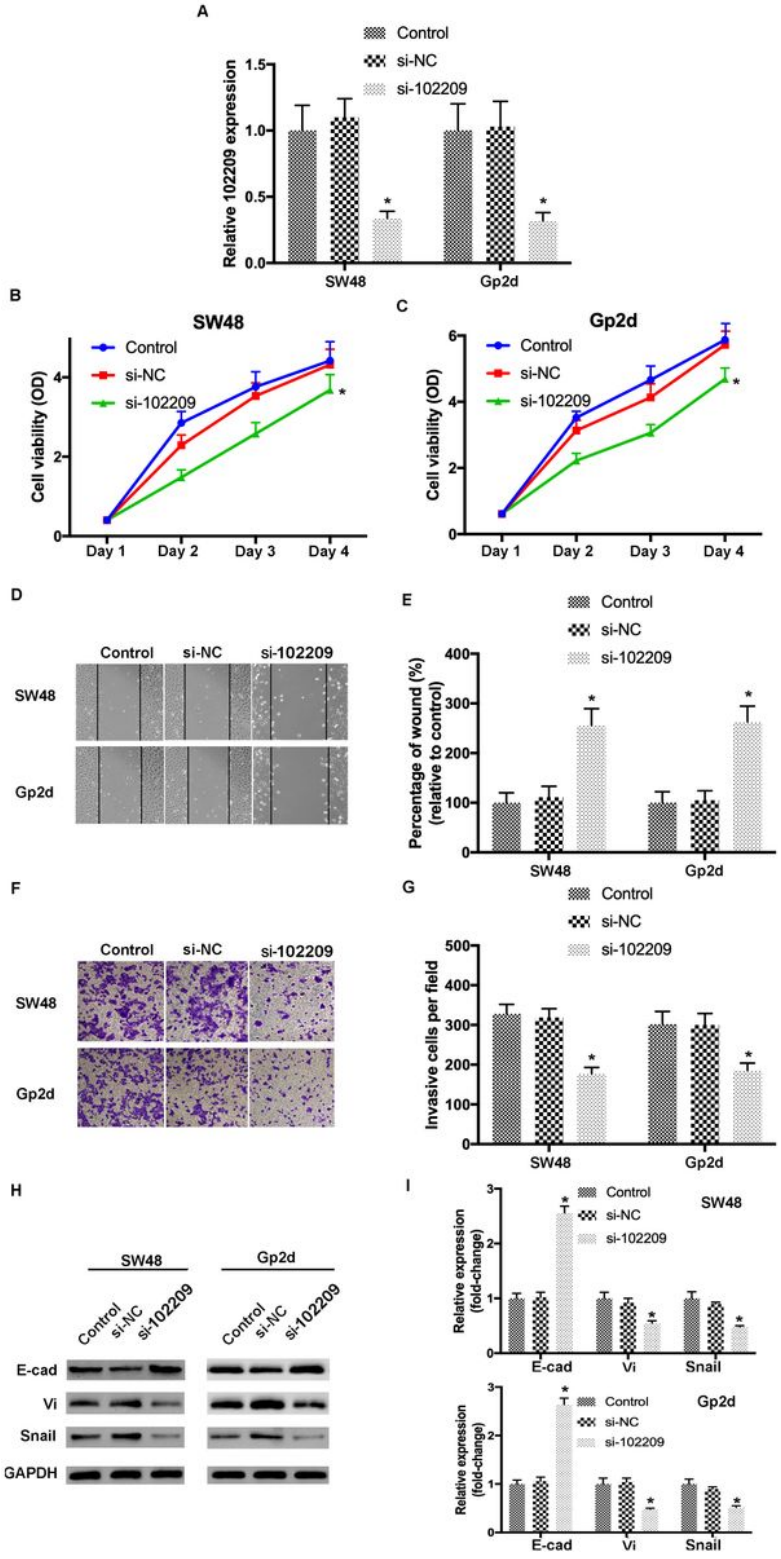

Figure 2

Knockdown of hsa_circ_102209 inhibits the proliferation, migration, invasion and EMT of CRC cells. (A) Transfection efficiency of si-hsa_circ_102209 was evaluated by reverse transcription-quantitative polymerase chain reaction. (B and C) The proliferative activity of CRC cells transfected with si-

hsa_circ_102209 or si-NC were examined using Cell Counting Kit-8 assay. (D and E) The migrating ability of transfected SW48 and Gp2d cells were determined by wound healing assay (magnificationx100). (F and G) The invasion of CRC cells transfected with si-hsa_circ_102209 or si-NC were evaluated (magnificationx200). (H and I) The levels of EMT-related molecules were assessed using both RT-qPCR and western blotting. *P<0.05. CRC, colorectal cancer; NC, negative control.

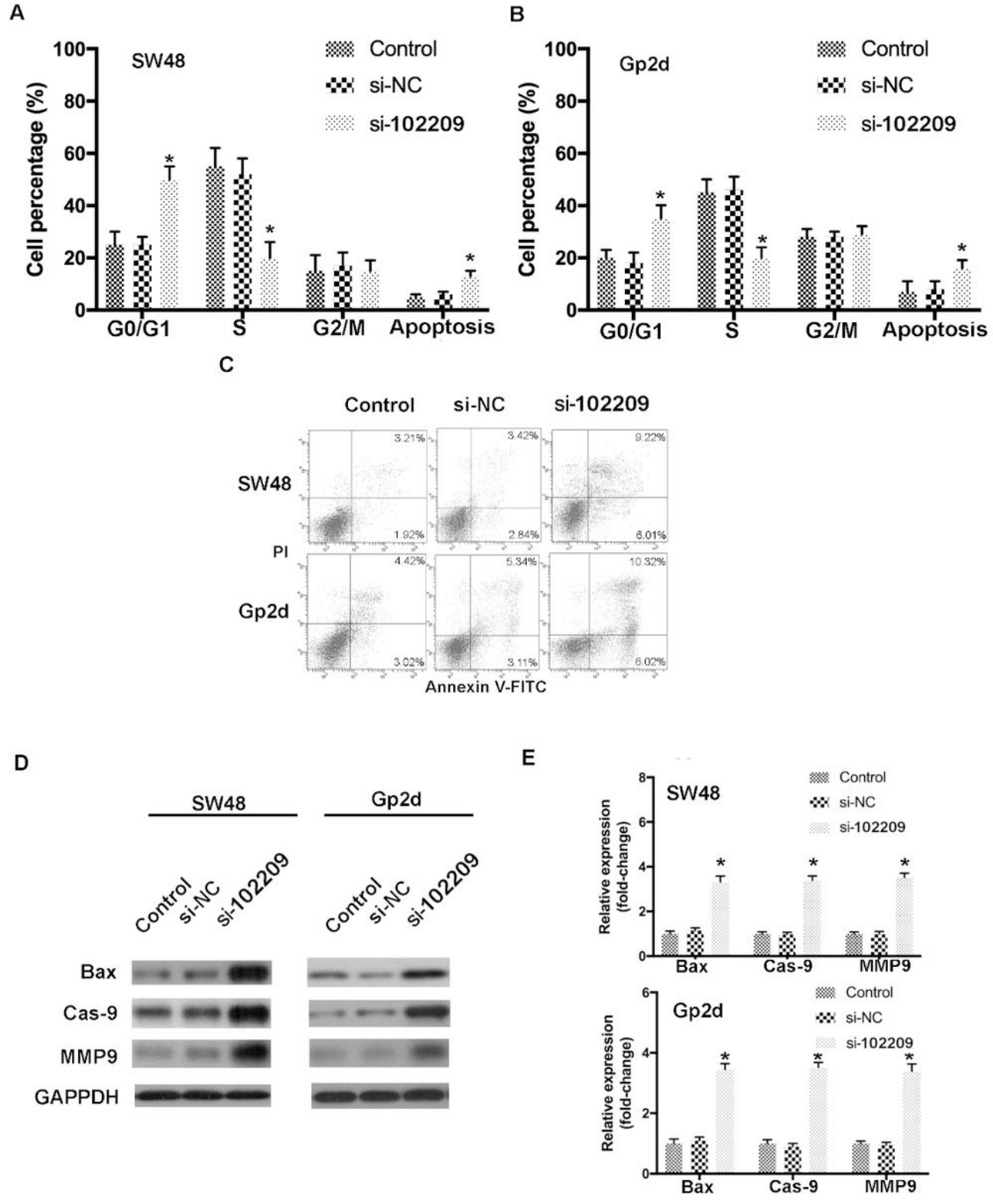

Figure 3

Knockdown of hsa_circ_102209 promotes cell cycle arrest and apoptosis in CRC cells. (A and B) The distribution of cell cycle and apoptosis of CRC cells with hsa_circ_102209 knockdown were evaluated. (C) The apoptosis of SW48 and Gp2d cells transfected with si-hsa_circ_102209 were also examined by flow cytometry. (D and E) The expression profile of apoptosis-related molecules were determined in CRC cells with hsa_circ_102209 knockdown compared to the control. *P<0.05. CRC, colorectal cancer.

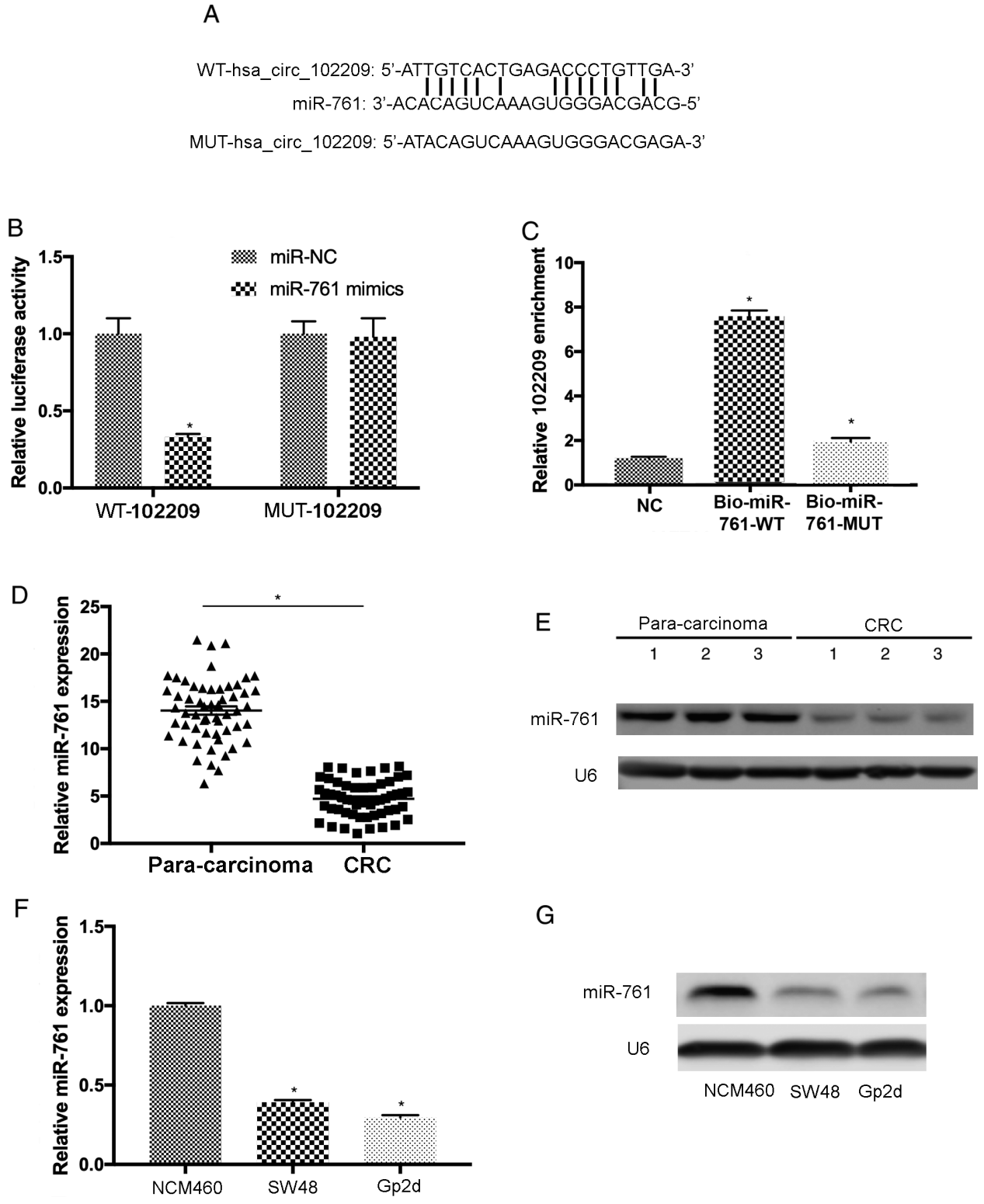

Figure 4

MiR-761 is the putative target of hsa_circ_102209 in CRC cells. (A) The complementary binding sites between hsa_circ_102209 and miR-761 were predicted. (B) The association of hsa_circ_102209 and miR-761 was further confirmed by luciferease reporter assay. (C) In RNA-pull-down assay, hsa_circ_102209 was enriched in biotin-labeled miR-761-WT group. (D to G) The expression levels of miR-761 were decreased in CRC clinical samples and cell lines. (*P<0.05. CRC, colorectal cancer; NC, negative control.

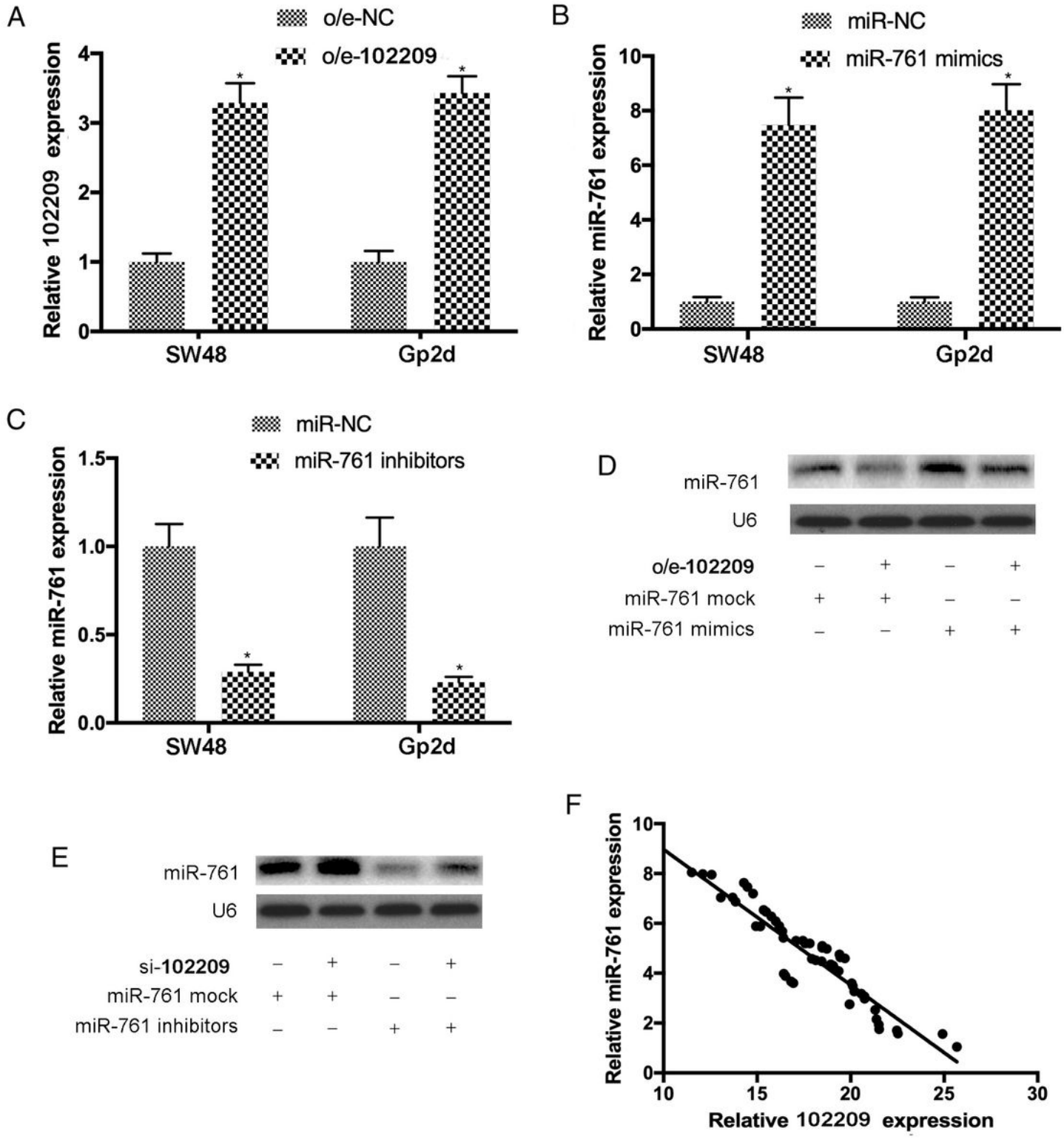

Figure 5

The expression of miR-761 was downregulated by hsa_circ_102209 in CRC. (A to C) The transfection efficiencies of o/e-102209, miR-761 mimics and inhibitors were confirmed by RT-qPCR. (D and E) The levels of miR-176 were negatively regulated by hsa_circ_102209 in CRC cells. (F) The expression of hsa_circ_102209 and miR-761 were inversely correlated in CRC samples (r=-0.3223; P=0.00909). *P<0.05. CRC, colorectal cancer.

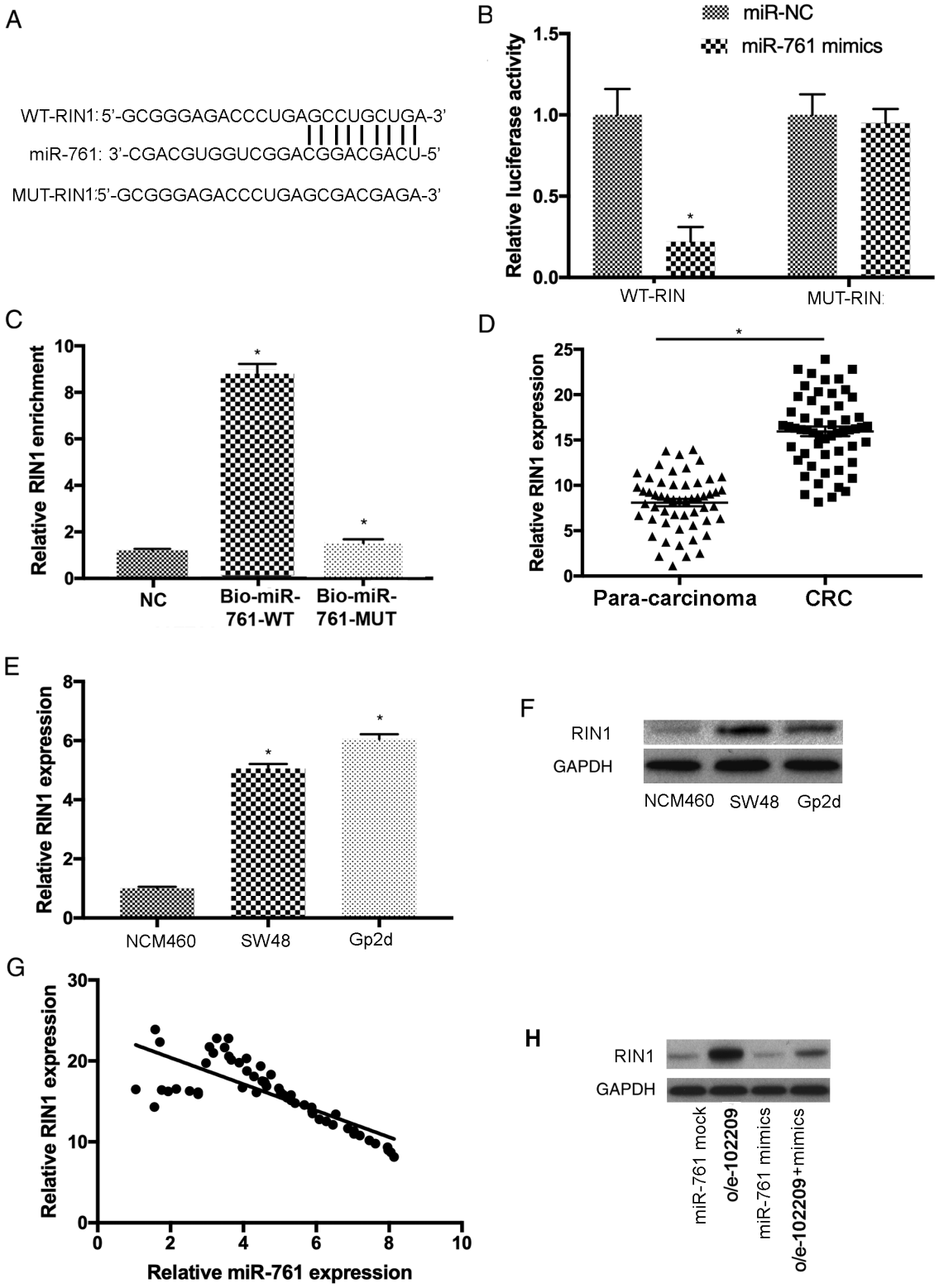

Figure 6

RIN1 is a novel downstream molecule of miR-761 in CRC cells. (A) The binding sites of RIN1 on the transcript of miR-761 were predicted. (B) The correlation between RIN1 and miR-761 was elucidated using luciferase activity assay. (C) In RNA-pull-down assay, hsa_circ_102209 was enriched in biotin-labeled miR-761-WT group. (D to F) RIN1 expression was elevated in both CRC tissues and cells. (G) The levels of RIN1 and miR-761 were inversely correlated in CRC (r=-0.3555; P=0.00912). (H) The levels of RIN1 were positively modulated by hsa_circ_102209 and negatively regulated by miR-761 in CRC cells. *P<0.05. CRC, colorectal cancer.

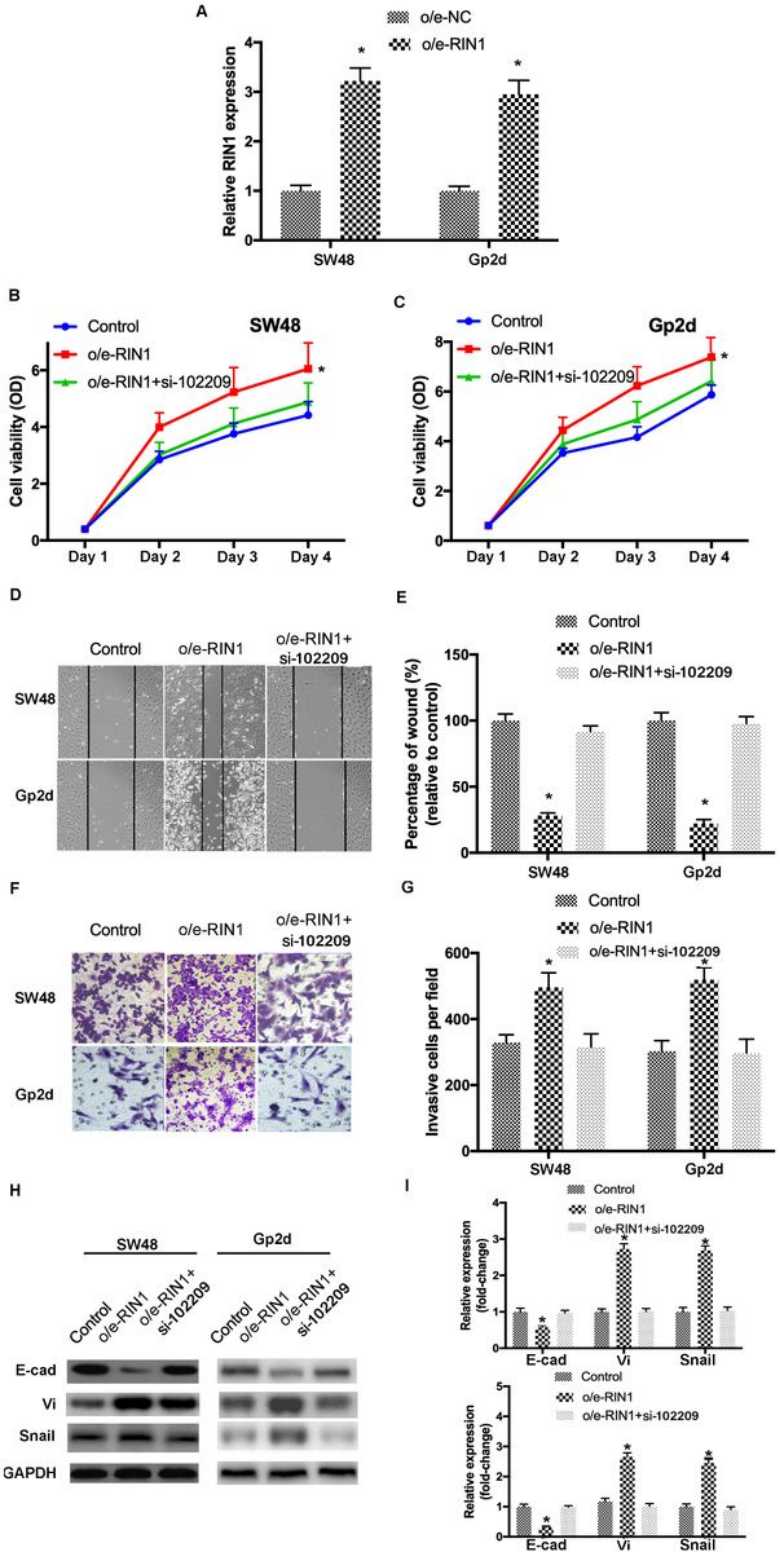

Figure 7

RIN1 could contribute to hsa_circ_102209-induced biological behavior changes in CRC cells. (A) The transfection efficiency of o/e-RIN1 was confirmed using RT-qPCR. (B-G) The proliferative, migrating and invasive activity of CRC cells was enhanced by o/e-RIN1, which was inhibited by si-hsa_circ_102209. (H and I) The levels of EMT-related were also determined in transfected CRC cells. *P<0.05. CRC, colorectal cancer; NC, negative control.

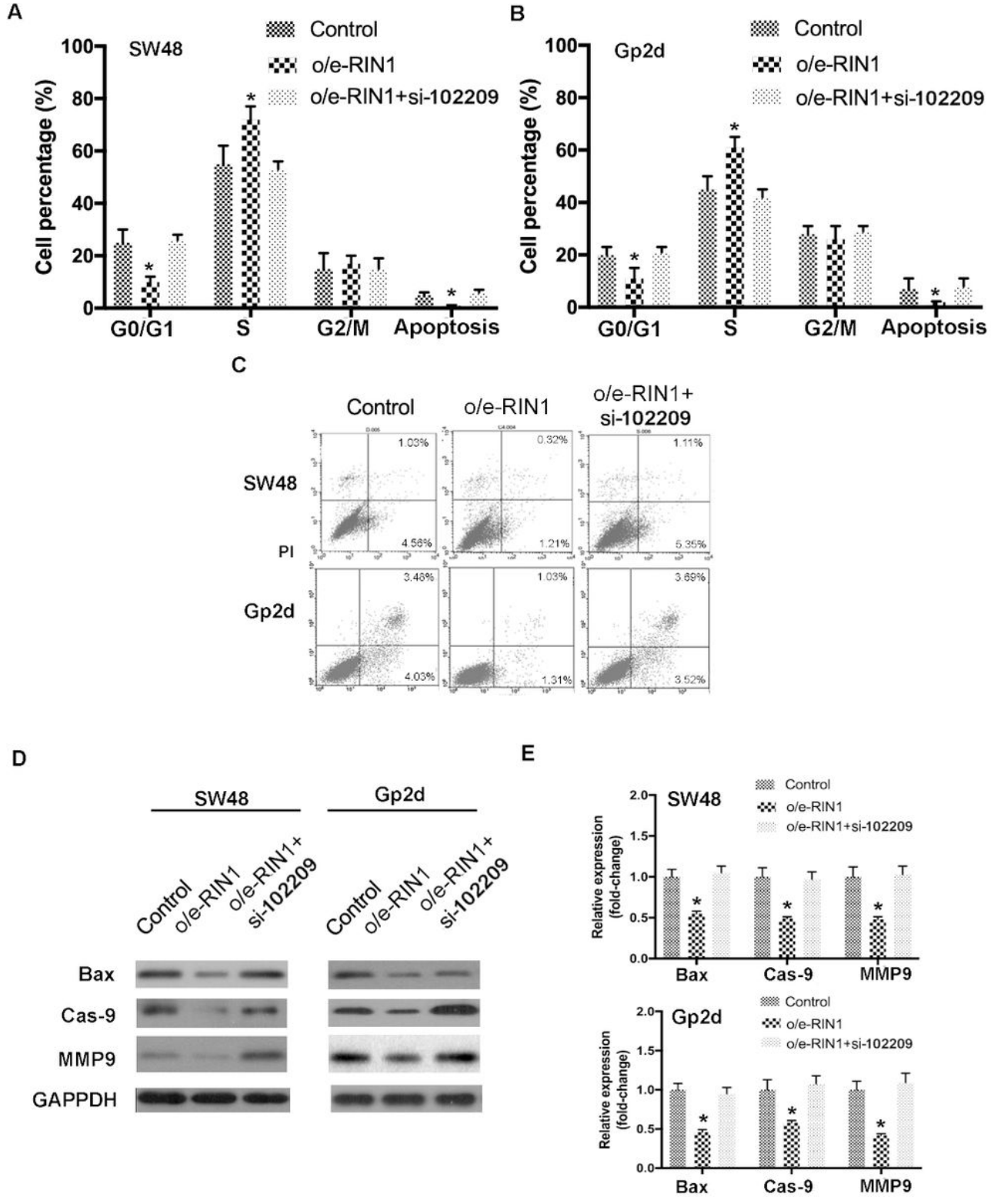

Figure 8

RIN1 is involved in hsa_circ_102209-modulated cell cycle arrest and apoptosis in CRC. (A and B) Overexpressed RIN1 suppressed cell cycle arrest in CRC cells, which was abrogated by hsa_circ_102209 knockdown. (C to E) The apoptosis of CRC cells was inhibited by the transfection of o/e-RIN1, and these effects were reversed by knockdown of hsa_circ_102209. *P<0.05. CRC, colorectal cancer.

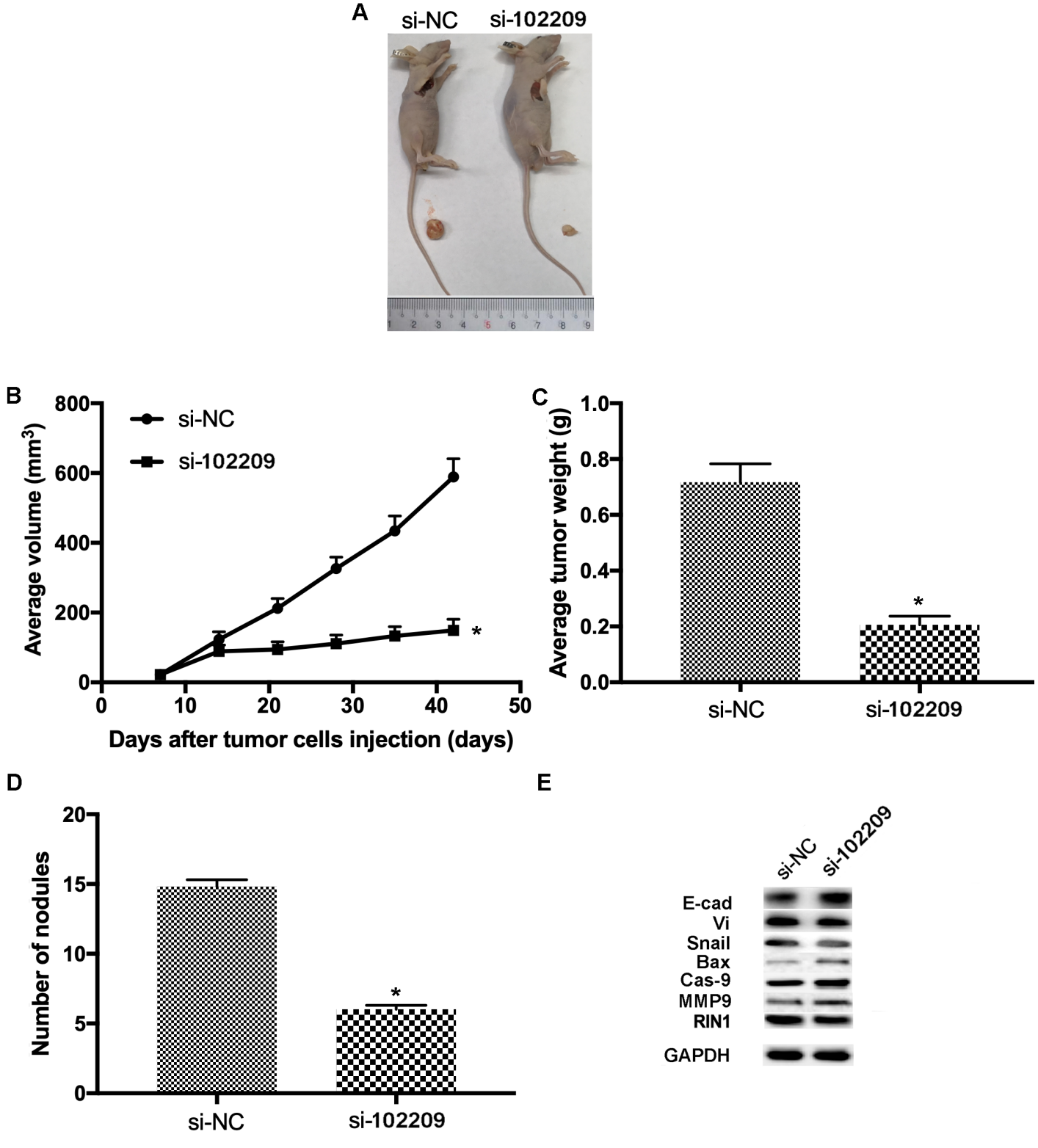

Figure 9

Knockdown of hsa_circ_102209 inhibited the development of CRC in mouse model. (A) Six weeks post-injection, the mice were sacrificed and tumor tissues were examined. (B and C) The average tumour weight and volume were both significantly reduced in hsa_circ_102209 knockdown mice. (D) The numbers of macroscopic nodules in hsa_circ_102209 knockdown group was also examined compared with the control. (E) The levels of EMT-/apoptosis-markers and RIN1 exhibited the same expression pattern as observed in the in vitro assays. *P<0.05. CRC, colorectal cancer; NC, negative control.